AGU PUBLICATIONS

Geophysical Research Letters

RESEARCH LETTER
10.1002/2016GL069293

Key Points:
- Extensive airborne measurements reveal widespread influence of waves on tropical high cirrus clouds
- Cirrus clouds preferentially occur at cold anomalies with ongoing cooling
- Vertical scales of waves affect vertical scales of cirrus layers

Supporting Information:
- Supporting Information S1

Correspondence to:
J.-E. Kim,
jieunk@colorado.edu

Citation:
Kim, J.-E., M. J. Alexander, T. P. Bui, J. M. Dean-Day, R. P. Lawson, S. Woods, D. Hlavka, L. Pfister, and E. J. Jensen (2016), Ubiquitous influence of waves on tropical high cirrus clouds, *Geophys. Res. Lett.*, *43*, 5895–5901, doi:10.1002/2016GL069293.

Received 22 APR 2016
Accepted 27 MAY 2016
Accepted article online 31 MAY 2016
Published online 11 JUN 2016

Ubiquitous influence of waves on tropical high cirrus clouds

Ji-Eun Kim[1,2], M. Joan Alexander[3], T. Paul Bui[4], Jonathan M. Dean-Day[5], R. Paul Lawson[6], Sarah Woods[6], Dennis Hlavka[7], Leonhard Pfister[4], and Eric J. Jensen[4]

[1]Earth System Research Laboratory, National Oceanic and Atmospheric Administration, Boulder, Colorado, USA, [2]Cooperative Institute for Research in Environmental Sciences, University of Colorado Boulder, Boulder, Colorado, USA, [3]NorthWest Research Associates, CoRA Office, Boulder, Colorado, USA, [4]NASA Ames Research Center, Moffett Field, California, USA, [5]Bay Area Environmental Research Institute, Petaluma, California, USA, [6]SPEC Inc., Boulder, Colorado, USA, [7]Science Systems and Applications, Inc., NASA Goddard Space Flight Center, Greenbelt, Maryland, USA

Abstract Cirrus clouds in the tropical tropopause layer (TTL) and water vapor transported into the stratosphere have significant impacts on the global radiation budget and circulation patterns. Climate models, however, have large uncertainties in representing dehydration and cloud processes in the TTL, and thus their feedback on surface climate, prohibiting an accurate projection of future global and regional climate changes. Here we use unprecedented airborne measurements over the Pacific to reveal atmospheric waves as a strong modulator of ice clouds in the TTL. Wave-induced cold and/or cooling conditions are shown to exert a nearly ubiquitous influence on cirrus cloud occurrence at altitudes of 14–18 km, except when air was very recently influenced by convective hydration. We further observe that various vertical scales of cloud layers are associated with various vertical scales of waves, suggesting the importance of representing TTL waves in models.

1. Introduction

Water vapor in the troposphere is the most abundant and strongest greenhouse gas [*Kiehl and Trenberth*, 1997]. The amount of water vapor in the stratosphere is highly limited, but the small amount still has an important greenhouse effect [*Dessler et al.*, 2013]. Recent trends and decadal variations in observed stratospheric water vapor have had radiative impacts on global surface temperature comparable to the warming caused by increasing greenhouse gases [*Forster and Shine*, 2002; *Solomon et al.*, 2010]. Stratospheric water vapor is transported upward through the tropical tropopause layer (TTL) by a slow rising motion, then poleward via the continuous large-scale meridional circulation of the global stratosphere [*Brewer*, 1949; *Fueglistaler et al.*, 2009]. The extremely cold TTL behaves like a filter, effectively freeze-drying the rising air through the process of ice cloud formation and sedimentation. Thus, the filtering efficiency depends on cloud processes in the TTL [*Jensen and Pfister*, 2004]. Interestingly, in addition to the role of stratospheric water vapor on global surface temperature, the radiative impact of water in the TTL itself strongly depends on the phase of water, mainly due to differences in infrared absorption between water vapor and ice crystals. Recent studies have shown that radiative impacts by tropical high-level ice clouds and water vapor in the upper troposphere and lower stratosphere play a critical role in shaping tropospheric circulation in models, affecting the strength of the Hadley cell, and the locations of the Intertropical Convergence Zone, extratropical jet streams, and storm tracks [*Maycock et al.*, 2013; *Voigt and Shaw*, 2015].

These important impacts of water in the TTL and stratosphere on climate emphasize the need to accurately represent TTL ice cloud processes in global climate models. However, there is a large spread in stratospheric water vapor concentrations and TTL cloud frequencies among models [*Gettelman et al.*, 2010; *Randel and Jensen*, 2013; *Hardiman et al.*, 2015]. A lack of observations limits our current understanding of the TTL dehydration process and the availability of constraints needed for better simulation of ice clouds in models. One of the processes involved in TTL dehydration and accompanying cirrus formation is wave-induced temperature variability. While a number of modeling studies have shown that waves affect cirrus clouds and dehydration in the TTL [e.g., *Potter and Holton*, 1995; *Jensen et al.*, 1996; *Luo et al.*, 2003; *Jensen and Pfister*, 2004; *Schoeberl and Dessler*, 2011; *Ueyama et al.*, 2015], only a handful of observational studies have suggested wave impacts on cloud occurrence [*Boehm and Verlinde*, 2000; *Pfister et al.*, 2001; *Immler et al.*, 2008; *Fujiwara et al.*, 2009]. Furthermore, the sampling in previous measurements was too limited to determine a robust relationship between cirrus and

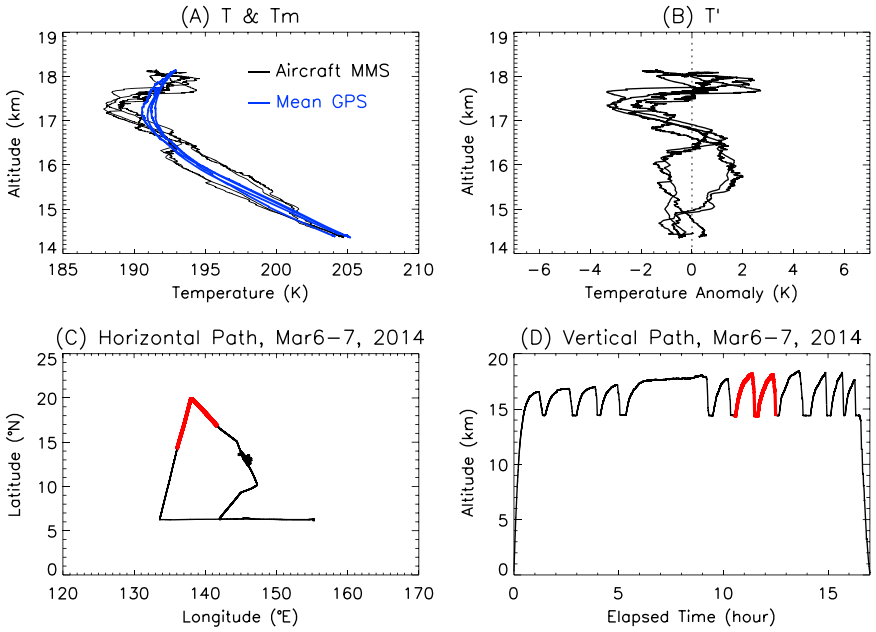

Figure 1. Example of temperature profiles and a horizontal and vertical path. (a) Vertical profiles are temperatures measured by the Meteorological Measurement System (MMS) on the aircraft (black) with corresponding GPS 30 day mean profiles (blue) and (b) temperature anomalies, MMS-GPS, for the flight segment at (c) the red horizontal and (d) red vertical path during the flight on 6–7 March 2014.

waves. In this study, we present evidence of dominant wave influence on ice cloud occurrence observed in the recent extensive survey of the TTL over the Pacific by NASA's unmanned aircraft, the Global Hawk, during the Airborne Tropical TRopopause EXperiment (ATTREX) [*Jensen et al.*, 2013, 2016].

2. Data and Methods

ATTREX investigators conducted a series of airborne measurements of high-altitude cirrus clouds: (a) over the tropical eastern Pacific in October–November 2011, (b) over the central and eastern Pacific in February–March 2013, and (c) over the western Pacific in February–March 2014. The measurements included temperatures [*Scott et al.*, 1990], ice particle properties [*McFarquhar et al.*, 2007], and cloud layer information [*McGill et al.*, 2002]. Long-duration flights with repeated vertical descent/ascent maneuvers between ~14 and ~18 km provided unprecedented observations of ice clouds in the TTL. Since aircraft measurements provide in situ temperatures (T) only, we need additional information about the mean temperature ($\overline{T}$) to calculate wave temperature anomalies $\left(T'=T-\overline{T}\right)$ along flight tracks. We utilized Global Positioning System (GPS) radio occultation data [*Kursinski et al.*, 1997; *Anthes et al.*, 2008] to provide accurate mean vertical temperature profiles.

For each 1 s interval of ATTREX aircraft measurements, we calculated the mean temperature by averaging GPS temperatures for 30 days and 10° × 5° (in longitude and latitude) centered on each flight time and location along the flight tracks. This procedure yields the same number of mean temperatures as in situ aircraft temperature data. Temperature anomalies with 1 s interval were calculated by subtracting GPS mean temperatures from aircraft temperatures (see Figure 1). Note that temperature anomalies are time anomalies at each vertical data point, so resulting anomaly profiles can be considered as waves (that is, the mean vertical temperature structure is already removed.). Since we used the 30 day time mean, the temperature anomalies were induced by waves at periods shorter than 30 days, including gravity, Kelvin, and mixed Rossby-gravity waves. All of these waves contribute to the determination of the cold point temperature [*Kim and Alexander*, 2015]. Over the ATTREX flight ranges, about 24 GPS profiles were averaged to calculate the mean temperature for each 1 s. Figures 1a and 1b show example temperature profiles from the aircraft (black in Figure 1a) and GPS mean temperatures (blue in Figure 1a) and anomalies in Figure 1b. Their corresponding segment of the aircraft path is shown with red in Figures 1c and 1d for the flight on 6–7 March 2014.

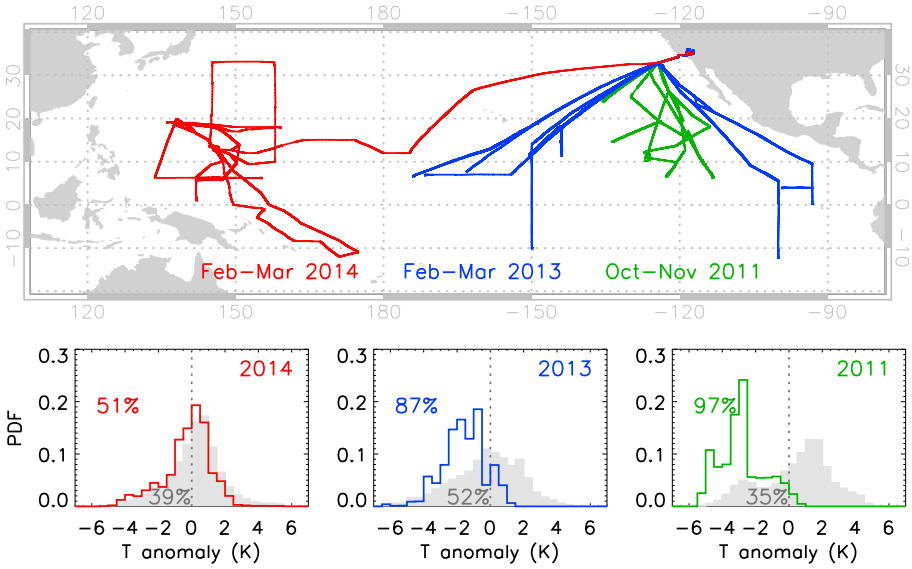

Figure 2. ATTREX flight tracks and PDFs of temperature anomalies for all-sky (grey) and cloudy (color) cases. Color lines in bottom plots are PDFs of temperature anomalies where cirrus clouds with ice particle number concentration higher than 30/L were observed. Data between 12°S–20°N and 14–18 km were used. A temperature anomaly is calculated by subtracting a 30 day GPS mean value from the aircraft measured temperature at 1 s intervals. Percentage represents the ratio of the number of negative temperature anomalies sampled to the total.

3. Results and Discussion

3.1. Relationship Between Temperature Anomalies and Cirrus Occurrence

The colored lines in the bottom plots in Figure 2 show probability density functions (PDFs) of temperature anomalies when ice clouds were observed at 14–18 km. Even though the total sampling in 2011 is skewed toward the positive anomaly side (grey PDF), 97% of clouds were observed where temperature perturbations were negative. The 2013 data also show a strong effect of waves, with 87% of clouds occurring in cold anomalies, while the total sampling displays an unbiased PDF.

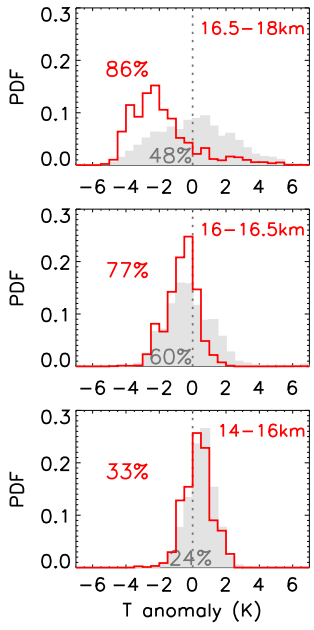

Figure 3. Same as the bottom left in Figure 2 but for different vertical ranges for 2014.

The relationship between temperature anomalies and clouds seems weak in the western Pacific 2014 data in Figure 2. For a more detailed analysis we divided the data into three vertical layers in Figure 3. The lower layer PDF shows little dependence on waves, while the middle layer shows a transitional behavior between the upper and lower layers. The upper layer (>16.5 km) clouds dominantly formed within cold anomalies (86%). Although cirrus cloud occurrence at these high altitudes is not very frequent (8% of 2014 measurements) compared to the lower altitude clouds (23%), impacts of these very high clouds are significant through their modulation of radiative forcing, either directly or through their effect on

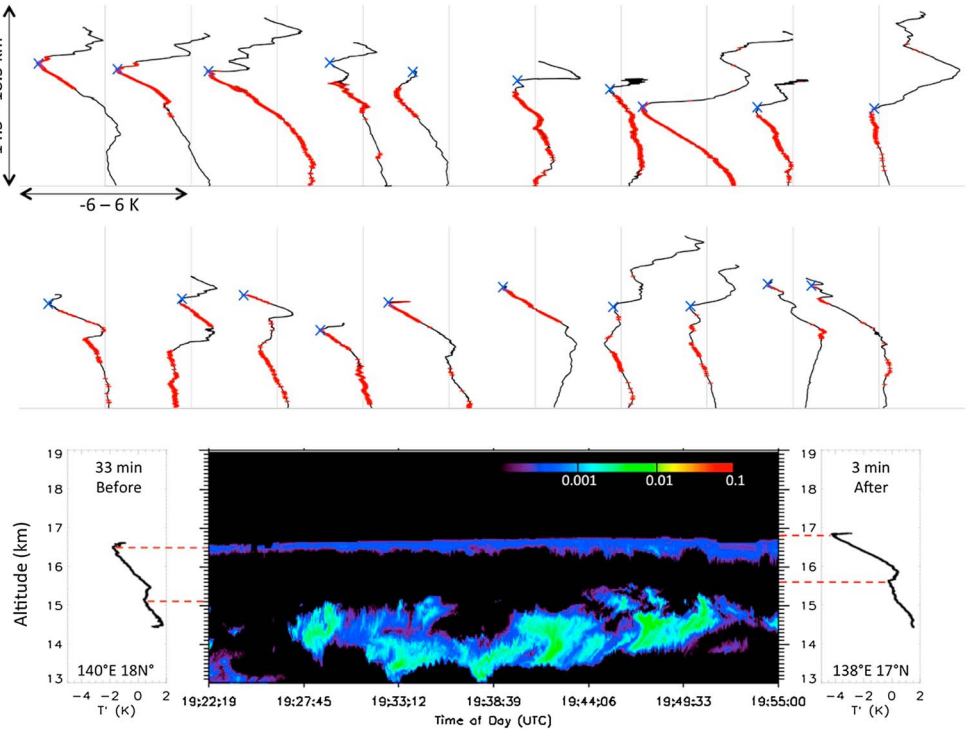

Figure 4. Examples of temperature anomaly profiles and clouds. (first and second rows) Black thick curves are the temperature anomalies during aircraft descents. The vertical thin straight line is for a zero anomaly, and the anomaly range in *x* axis is overlapped. Red areas represent the observed ice clouds. A height for the minimum observed temperature in each profile is marked by blue cross. (third row) Cloud layers were detected by attenuated backscatter from 1064 nm lidar scans between two aircraft descents on 4 March 2014. The left anomaly profile was measured before the beginning of the cloud lidar measurements, and the right anomaly profile was measured after turning off the lidar.

water vapor. Slowly rising air in this extremely cold layer at 16.5–18 km experiences a final dehydration before it enters into the warmer stratosphere. The strong correlation we observe between clouds and negative temperature anomalies supports the previous idea that waves regulate lower stratospheric water vapor by lowering cold point temperatures in the TTL [*Kim and Alexander*, 2015].

3.2. Vertical Profiles of Waves and Cirrus Observed During Aircraft Descents

Vertical profiling of aircraft measurements provides an excellent opportunity to observe more detailed wave structures and cloud characteristics. Compared to ascents, descents of the aircraft throughout the TTL layer happen very quickly, usually within ~10 min and within a 1° × 1° horizontal area; thus, aircraft descents provide dropsonde-like measurements. Figure 4 shows examples of vertical profiles of temperature anomalies (black) when ice particles (red) were observed during descents. The profiles in the top plots show that a cloud layer (red) is roughly capped by a peak of a negative wave phase, which is often the same as the cold point tropopause (blue "cross" mark). Since the black curves are anomaly (T') profiles, not temperature (T) profiles, the cold point tropopause is not necessarily the same as the minimum point of the profiles in Figure 4. However, when waves have a cold phase near the mean tropopause, clouds are more likely to form as the minimum temperature gets even colder than the mean condition, and wave-induced cold anomalies often coincide with the cold point tropopause [*Kim and Alexander*, 2015]. While we show cloud layers that are associated with relatively deep vertical wave structures (wavelengths $>$ ~4 km) in the first row in Figure 4, the examples in the second row show that the wave-cloud relationship also holds at shorter vertical scales. In some cases, very thin cloud layers are associated with shallow waves at wavelengths as short as ~300 m. The profiles indicate that multiple layers of these thinnest clouds can exist due to multiple layers of shallow waves, which cannot be resolved in current global climate and analysis models due to limited vertical resolution.

The general relationship between waves and clouds in Figure 4 indicates not only that the cold or warm phase is important but also that changes between wave phases determine cloud occurrence. Clouds were

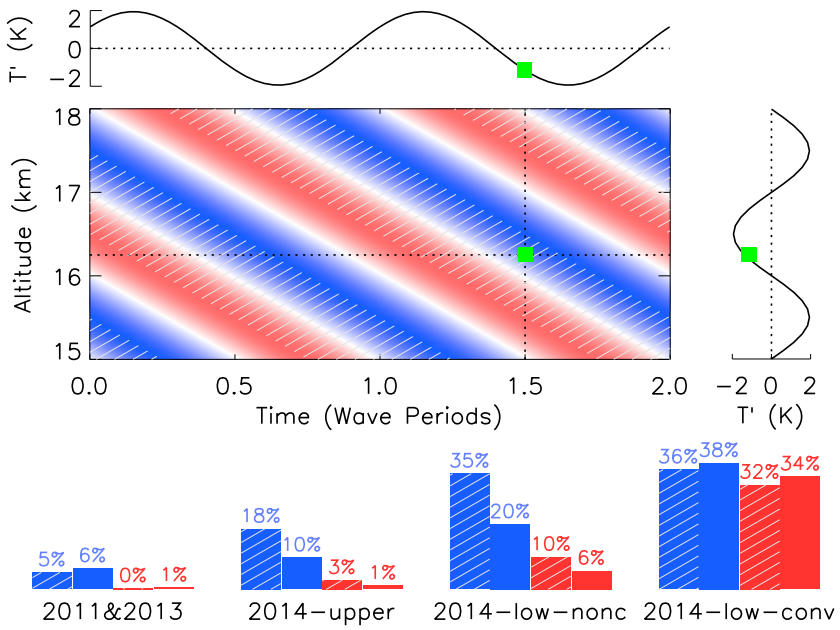

Figure 5. Schematic of a temperature anomaly pattern induced by a wave in the TTL and cloud occurrence frequency measured during ATTREX for different wave phases. The color shading represents the temperature anomalies (red: $T' > 0$, blue: $T' < 0$). The hatching represents the negative vertical gradients of temperature anomalies ($dT'/dz < 0$). At any given point (green square in this example), a negative vertical slope ($dT'/dz < 0$) corresponds to a negative time derivative ($dT'/dt < 0$). (bottom) Bar charts are for ice cloud occurrence frequency of 2 m vertical binned data from aircraft descents. Four categories of wave phases are (i) $T' < 0$ and $dT'/dz < 0$ with blue and hatching, (ii) $T' < 0$ and $dT'/dz > 0$ with solid blue, (iii) $T' > 0$ and $dT'/dz < 0$ with red and hatching, and (iv) $T' > 0$ and $dT'/dz > 0$ with solid red. From the left to right, results are for an average between 2011 and 2013, high-altitude (>16.5 km) sampling in 2014, low-altitude (<16 km) nonconvective cases in 2014, and low-altitude convectively influenced cases in 2014 (supporting information).

more often observed at a negative vertical slope of temperature anomalies (i.e., $dT'/dz < 0$) than a positive slope. A combination of in situ aircraft measurements during descents and lidar profiles between the descents provides a good example of cloud layers in relation to temperature perturbations, as shown in the bottom plot of Figure 4. We can observe that highest, thinnest clouds follow roughly the peaks of negative temperature anomalies and negative slopes (see layer at ~16.5 km ➔ ~16.7 km) and that cloud layers have a gap near where positive slopes and positive temperature anomalies occur.

3.3. Indication of Importance of Cooling Rates

We propose a probable reason that a negative slope in the temperature anomaly profiles provides a favorable condition for cloud occurrence in the schematic in Figure 5. Since the main wave source is tropical convection below, energy goes upward while wave phase progresses downward in the TTL. The wave phase progression accompanies the temperature anomaly pattern shown in Figure 5, moving downward with time. This is a very typical wave anomaly structure in the TTL, which can be observed in radiosonde observations [e.g., *Boehm and Verlinde*, 2000; *Kim and Alexander*, 2015; *Jensen et al.*, 2016]. In our analysis, one wave period could have any value between a few minutes to 30 days. Based on this general wave structure, the sign of dT'/dt (time derivative) can be deduced only from dT'/dz (vertical slope). For instance, at a certain point (green square), dT'/dt will have the same sign as dT'/dz. This relationship holds at any point if anomalies were caused by an upward propagating wave. Therefore, the preferential cloud occurrence at $dT'/dz < 0$ implies that cirrus clouds preferentially form and exist when a local air parcel experiences cooling, $dT'/dt < 0$.

4. Summary and Conclusion

The bar charts in Figure 5 provide a comprehensive summary of cirrus cloud properties from the all ATTREX measurements. Using vertical profiles during aircraft descents, cloud occurrence frequency (in percentage) was calculated for four categories depending on the sign of T' and dT'/dz. Over the central and eastern Pacific, cirrus clouds are infrequent, but they almost always form in the cold phase of a wave. We note that,

compared to the eastern Pacific statistics for altitudes of 14–18 km in Figure 5, cloud occurrence frequency over the eastern Pacific especially for 2011 is increased if we only take samplings at altitudes of 14–17 km, as suggested in Figure S1 in the supporting information. Regardless of the change in cloud occurrence frequency with different vertical sampling ranges, the importance of the cold wave phase for cirrus occurrence remains the same. Since cirrus clouds in the lower TTL (14–16 km) over the western Pacific could be under the combined influence of waves and convective moisture transport, we divided the western Pacific measurements into three groups: the upper TTL, nonconvective lower TTL, and convectively influenced lower TTL. The convective and nonconvective cases were decided based on nearby convection penetrating to TTL altitudes as observed by geostationary satellite data (supporting information). The statistics in Figure 5 show that, without the presence of nearby deep convection, the wave cold phase ($T < 0$) with ongoing wave cooling ($dT'/dt < 0$) is the best condition for cirrus occurrence. This wave-cirrus relationship is particularly prevalent in the uppermost TTL over the western Pacific where most tropospheric air enters the stratosphere [*Fueglistaler et al*., 2004], indicating an important role of waves on stratospheric water vapor transport.

To our knowledge, this is the first study presenting direct observational evidence for such ubiquitous influence of wave-induced cold anomalies and cooling rates on cirrus cloud occurrence. Although more observations will still be needed, the advancement in understanding of ice clouds in the TTL presented here will provide guidance for future measurements and a simple methodology for evaluating climate models that can lead to improvements in representations of waves, cirrus clouds, and their feedback on surface climate.

Acknowledgments

Data are available at https://espoarchive.nasa.gov/archive/browse/attrex (ATTREX) and http://cdaac-www.cosmic.ucar.edu/cdaac/products.html (COSMIC GPS). We thank two reviewers for their helpful comments that improved the manuscript. This work was supported by NASA Ames Research Center contract NNA10DF70C as part of the Airborne Tropical TRopopause EXperiment (ATTREX) under the NASA Science Mission Directorate Earth Venture Program.

References

Anthes, R. A., et al. (2008), The COSMIC/FORMOSAT-3 mission: Early results, *Bull. Am. Meteorol. Soc.*, *89*, 313–333.

Boehm, M. T., and J. Verlinde (2000), Stratospheric influence on upper tropospheric tropical cirrus, *Geophys. Res. Lett.*, *27*, 3209–3212, doi:10.1029/2000GL011678.

Brewer, A. W. (1949), Evidence for a world circulation provided by the measurements of helium and water vapor distribution in the stratosphere, *Q. J. R. Meteorol. Soc.*, *75*, 351–363.

Dessler, A. E., M. R. Schoeberl, T. Wang, S. M. Davis, and K. H. Rosenlof (2013), Stratospheric water vapor feedback, *Proc. Natl. Acad. Sci. U.S.A.*, *110*(45), 18,087–18,091.

Forster, P. M., and K. P. Shine (2002), Assessing the climate impact of trends in stratospheric water vapor, *Geophys. Res. Lett.*, *29*(6), 1086, doi:10.1029/2001GL013909.

Fueglistaler, S., H. Wernli, and T. Peter (2004), Tropical troposphere-to-stratosphere transport inferred from trajectory calculations, *J. Geophys. Res.*, *109*, D03108, doi:10.1029/2003JD004069.

Fueglistaler, S., A. E. Dessler, T. J. Dunkerton, I. Folkins, Q. Fu, and P. W. Mote (2009), Tropical tropopause layer, *Rev. Geophys.*, *47*, RG1004, doi:10.1029/2008RG000267.

Fujiwara, M., et al. (2009), Cirrus observations in the tropical tropopause layer over the western Pacific, *J. Geophys. Res.*, *114*, D09304, doi:10.1029/2008JD011040.

Gettelman, A., et al. (2010), Multimodel assessment of the upper troposphere and lower stratosphere: Tropics and global trends, *J. Geophys. Res.*, *115*, D00M08, doi:10.1029/2009JD013638.

Hardiman, S. C., et al. (2015), Processes controlling tropical tropopause temperature and stratospheric water vapor in climate models, *J. Clim.*, *28*, 6516–6355.

Immler, R., K. Krüger, M. Fujiwara, G. Verver, M. Rex, and O. Schrems (2008), Correlation between equatorial Kelvin waves and the occurrence of extremely thin ice clouds at the tropical tropopause, *Atmos. Chem. Phys.*, *8*, 4019–4026.

Jensen, E. J., and L. Pfister (2004), Transport and freeze-drying in the tropical tropopause layer, *J. Geophys. Res.*, *109*, D02207, doi:10.1029/2003JD004022.

Jensen, E. J., O. B. Toon, L. Pfister, and H. B. Selkirk (1996), Dehydration of the upper troposphere and lower stratosphere by subvisible cirrus clouds near the tropical tropopause, *Geophys. Res. Lett.*, *23*, 825–828, doi:10.1029/96GL00722.

Jensen, E. J., G. S. Diskin, P. Lawson, S. Lance, T. P. Bui, D. Hlavka, M. McGill, L. Pfister, O. B. Toon, and R. Gao (2013), Ice nucleation and dehydration in the tropical tropopause layer, *Proc. Natl. Acad. Sci. U.S.A.*, *110*, 2041–2046.

Jensen, E. J., et al. (2016), The NASA Airborne Tropical TRopopause EXperiment (ATTREX): High-altitude aircraft measurements in the tropical western Pacific, *Bull. Am. Meteorol. Soc.*, doi:10.1175/BAMS-D-14-00263.1, in press.

Kiehl, J. T., and K. E. Trenberth (1997), Earth's annual global mean energy budget, *Bull. Am. Meteorol. Soc.*, *78*, 197–208.

Kim, J.-E., and M. J. Alexander (2015), Direct impacts of waves on tropical cold point tropopause temperature, *Geophys. Res. Lett.*, *42*, 1584–1592, doi:10.1002/2014GL062737.

Kursinski, E. R., G. A. Hajj, J. T. Schofield, R. P. Linfield, and K. R. Hardy (1997), Observing Earth's atmosphere with radio occultation measurements using the Global Positioning System, *J. Geophys. Res.*, *102*(D19), 23,429–23,465, doi:10.1029/97JD01569.

Luo, B. P., et al. (2003), Dehydration potential of ultrathin clouds at the tropical tropopause, *Geophys. Res. Lett.*, *30*(11), 1157, doi:10.1029/2002GL016737.

Maycock, A. C., M. M. Joshi, K. P. Shine, and A. A. Scaife (2013), The circulation response to idealized changes in stratospheric water vapor, *J. Clim.*, *26*, 545–561.

McFarquhar, G. M., J. Um, M. Freer, D. Baumgardner, G. L. Kok, and G. Mace (2007), The importance of small ice crystals to cirrus properties: Observations from the Tropical Warm Pool International Cloud Experiment (TWP-ICE), *Geophys. Res. Lett.*, *34*, L13803, doi:10.1029/2007GL029865.

McGill, M., D. Hlavka, W. Hart, V. S. Scott, J. Spinhirne, and B. Schmid (2002), Cloud physics lidar: Instrument description and initial measurement results, *Appl. Opt.*, *41*, 3725–3734.

Pfister, L., et al. (2001), Aircraft observations of thin cirrus clouds near the tropical tropopause, *J. Geophys. Res.*, *106*, 9765–9786, doi:10.1029/2000JD900648.

Potter, B. E., and J. R. Holton (1995), The role of monsoon convection in the dehydration of the lower tropical stratosphere, *J. Atmos. Sci.*, *52*, 1034–1050.

Randel, W. J., and E. J. Jensen (2013), Physical processes in the tropical tropopause layer and their roles in a changing climate, *Nat. Geosci.*, *6*, 169–176.

Schoeberl, M. R., and A. E. Dessler (2011), Dehydration of the stratosphere, *Atmos. Chem. Phys.*, *11*, 8433–8446.

Scott, S. G., T. P. Bui, K. R. Chan, and S. W. Bowen (1990), The meteorological measurement system on the NASA ER-2 aircraft, *J. Atmos. Oceanic Technol.*, *7*, 525–540.

Solomon, S., K. H. Rosenlof, R. W. Portmann, J. S. Daniel, S. M. Davis, T. J. Sanford, and G. K. Plattner (2010), Contributions of stratospheric water vapor to decadal changes in the rate of global warming, *Science*, *327*, 1219–1223.

Ueyama, R., E. J. Jensen, L. Pfister, and J.-E. Kim (2015), Dynamical, convective, and microphysical control on wintertime distributions of water vapor and clouds in the tropical tropopause layer, *J. Geophys. Res. Atmos.*, *120*, 10,483–10,500, doi:10.1002/2015JD023318.

Voigt, A., and T. A. Shaw (2015), Circulation response to warming shaped by radiative changes of clouds and water vapour, *Nat. Geosci.*, *8*, 102–106.